



## Pressure effects on solvation structure and dynamics in mixture of *cis* and *trans*-N-methylformamide in a protic and aprotic polar solvent

Apramita Chand and Snehasis Chowdhuri\*

School of Basic Sciences, Indian Institute of Technology, Bhubaneswar-752 050, Odisha, India

E-mail: snehasis@iitbbs.ac.in

Manuscript received online 08 May 2019, revised and accepted 22 May 2019

We have explored the effects of variation of pressure on solvation structure, dynamics and hydrogen bonding properties in mixture of *cis* and *trans*-N-methylformamide in protic/aprotic medium through classical molecular dynamics simulations. Hydrogen bonding preferences of  $O_{\text{NMF}}-H_{\text{NMF}}$  vary with *cis-cis/trans-trans/cis-trans/trans-cis* combinations but are overall better in DMSO solution than in aqueous solution. In both water/DMSO solutions, at  $X_{\text{NMF}} = 0.5$ , the *Ocis-Hcis* hydrogen bonding probability is enhanced which is boosted at higher pressures. Higher pressures may induce hydrogen bond contacts at intermediate pressures due to close packing but distortion in hydrogen bond network renders such hydrogen bonds less stable. *Cis*-NMF molecules prefer hydrogen bonding interactions with oxygen of DMSO while *trans*-NMF molecules engage their N-methyl groups for hydrophobic interactions with DMSO methyl groups. The disparity between *cis* and *trans*-NMF dipole rotations becomes more apparent in aqueous medium at higher pressures and higher NMF concentrations while difference in diffusion coefficients is significant at lower pressures. Higher lifetimes of  $O_{\text{DMSO}} \cdots H_{\text{cis}}$  hydrogen bonds may be responsible for longer dipole relaxation rates of *cis*-NMF in DMSO solution as pressure increases.

Keywords: *cis* and *trans*-NMF mixture, self-diffusion, orientational relaxation, hydrogen bond lifetime.

### 1. Introduction

Pressure variation is an important factor in determining structural changes in peptides and proteins in solution. Cumulative effects of pressure on various molecular interactions, particularly hydrogen bonding, influence denaturing/stabilizing effects on overall protein structure. It is well-established that hydration of proteins, hydrophobic interactions, van der Waals forces as well as solvent dynamics may be tuned by application of pressure<sup>1</sup>. In this context, it is exciting to gain atomistic level understanding of whether pressure modifies behaviour of peptide bonds in different solvent environments.

Conventionally, peptide bonds have been found to adopt the *trans*-conformation but it has been suggested in literature that *cis*-peptide bonds, which are thought to be sterically unfavourable, are possibly not detected properly due to limitations of existing techniques<sup>2</sup>. The vital role of *cis*-peptide bonds in influencing protein structure and function has been elucidated in several studies<sup>3-6</sup>. In order to microscopically examine pressure effects on *cis*- and *trans*-peptide

bonds in aqueous and non-aqueous solvent environments, a simple amide like N-methylformamide is suitable which is often chosen as a model peptide and has been sufficiently studied with respect to structural features of its *cis*- and *trans*-conformers<sup>7-12</sup>. The first theoretical study predicting various features of liquid mixture of *cis/trans* conformers of NMF was carried out by Skarmoutsos and Samios<sup>13</sup> where an idea of hydrogen bonding structure and dynamics in neat NMF was presented.

Properties like isothermal compressibility and self-diffusion in liquid NMF have been studied with varying pressures upto 200–300 MPa<sup>14</sup>. Chen and co-workers<sup>15,16</sup> varied pressures upto 200 MPa with different temperatures by employing spin-echo methods and observed retarded translational dynamics for *cis*-conformers relative to *trans*-NMF in liquid. As NMF is a reputed anti-tumour agent<sup>17,18</sup> and also interacts with bio-molecules, it is useful to comprehend how pressure may affect behavioural attributes of mixture of its conformations in solution.

Aqueous solutions of NMF have been widely inspected

with reference to viscosity, density, hydrogen bonding networks and dynamics by experimental<sup>19–22</sup> as well as theoretical methods<sup>23–27</sup>. Gerathanassis *et al.*<sup>28</sup> have combined <sup>17</sup>O-NMR experiments with theoretical approaches to explore hydration of *cis* and *trans*-NMF where it has been proposed that while both conformers are equally solvated by water with similar hydrogen bonding strength, the nature and extent of hydrogen bonding may differ depending on particular conformer sites. From DFT calculations, Wang and co-workers<sup>23</sup> noted that the complexes formed by *trans*-NMF and water are open, while those formed by *cis*-NMF and water are cyclic. Caminati and co-workers<sup>29</sup> have examined the rotational spectrum of NMF-water mixtures and have tried to find how water links differently to *cis* and *trans*-conformers. It was shown that *trans* conformers form either C=O...H-O or N-H...O hydrogen bonds while these bonds can co-exist in the *cis*-form when hydrogen bonded to water. It was also admitted that experimental limitations and the low abundance of the *cis*-conformers made it difficult to detect the *cis*-complexes even though *cis*-NMF-water adducts were reasonably stable as predicted by theoretical calculations.

The choice of DMSO for investigating pressure-effects on *cis-trans* mixture of NMF in non-aqueous milieu is compelling since DMSO is not only known for its diverse activity on protein structure but is also a versatile cryoprotectant, anti-oxidant and organic reagent<sup>30–32</sup>. Both NMF and DMSO have been demonstrated to be efficient as chemo-preventive agents against mammary cancer<sup>33</sup>. Dielectric studies of binary mixture of DMSO and NMF by Sengwa *et al.*<sup>34</sup> suggest that DMSO may act as 'structure breaker' in liquid NMF, with 2:1 NMF-DMSO complex formation which results in higher magnitude of excess dielectric properties. Quasi-ideality of NMF-DMSO liquid mixture around 50% DMSO concentration was proposed by Codeiro and Bosso<sup>35</sup> from interaction energy and excess enthalpy values obtained from Monte Carlo simulations. Combined neutron diffraction experiments and EPSR (electrostatic potential simulation refinement) simulations by Cordeiro and Soper<sup>36,37</sup> have demonstrated extensive solvation of NMF in DMSO with NMF-DMSO dimers which impart significant orientational structuring to the liquid. According to Borges and Cordeiro<sup>38</sup>, DMSO is a potential winner in the competition with water for NMF amide hydrogen since solvation shells are better organized with stronger hydrogen bonding in the NMF-DMSO mixture than in the aqueous solution.

In either water or DMSO medium, interactions of *cis*- and *trans*-NMF conformers have not been properly understood. In this study, we have presented a series of molecular dynamics simulations highlighting salient features of solvation and dynamics of two different conformers of NMF at two different protic/aprotic media (water/DMSO) compositions ( $X_{\text{NMF}} = 0.2$  and  $0.5$ ) along with variation of pressure.

## 2. Models and simulations

In the present work, *cis/trans* NMF and solvents (water/DMSO) molecules are characterized by the multisite interaction models. In these models, the interaction between atomic sites of two molecules is expressed as

$$u(r_{ij}) = 4\epsilon_{ij} \left[ \left( \frac{\sigma_{ij}}{r_{ij}} \right)^{12} - \left( \frac{\sigma_{ij}}{r_{ij}} \right)^6 \right] + \frac{q_i q_j}{r_{ij}} \quad (1)$$

where,  $q_i$  is the charge of the  $i$ -th atom or ion. The Lennard-Jones parameters  $\sigma_{ij}$  and  $\epsilon_{ij}$  are obtained by using the combination rules  $\sigma_{ij} = (\sigma_i + \sigma_j)/2$  and  $\epsilon_{ij} = \sqrt{\epsilon_i \epsilon_j}$ , where  $\sigma_i$  and  $\epsilon_i$  are the Lennard-Jones diameter and well-depth parameter for  $i$ -th atom. The hydrogen atoms of the methyl group are considered explicitly here. The rigid geometry and the values of the potential parameters  $q_i$ ,  $\sigma_i$ , and  $\epsilon_i$  for *cis* and *trans*-NMF as well as water and DMSO (P1 and P2 models) are taken from the literature<sup>13,39,40</sup>. The corresponding potential parameters are also summarized in Table 1.

Molecular dynamics simulations were carried out in a cubic box with a total of 500 particles consisting of NMF and solvent (either water or DMSO) molecules in three different compositions;  $X_{\text{NMF}} = 0.04$  (1 *trans*-NMF and 499 water/DMSO molecules),  $X_{\text{NMF}} = 0.2$  (6 *cis*-NMF, 94 *trans*-NMF and 400 water/DMSO molecules) and  $X_{\text{NMF}} = 0.5$  (15 *cis*-NMF, 235 *trans*-NMF and 250 water/DMSO molecules). The P2 model of DMSO has been preferably used in this work though the P1 model has also been considered for the sake of comparison. Six different pressures ranging from 0.1 MPa to 350 MPa, at a fixed temperature of 298 K were employed to perform the simulations. We have employed the minimum image convention for calculation of the short-range Lennard-Jones interactions. The long-range electrostatic interactions were treated using the Ewald method<sup>41</sup> in which the real space portion of the Ewald sum was evaluated by employing a spherical cutoff at  $0.5L$ , where  $L$  is the edge length of the

**Table 1.** Values of Lennard-Jones and electrostatic interaction potential parameters for *cis* and *trans*-NMF

Name	Atom/Ion	$\sigma$ (Å)	$\epsilon$ (K)	Charge	
				( $e_{cis}$ )	( $e_{trans}$ )
NMF	C	3.70	50.0	0.470	0.420
	H(C)	2.30	11.0	0.060	0.060
	O	2.96	80.0	-0.510	-0.524
	N	3.25	8.0	-0.510	-0.496
	H(N)	2.30	50.0	0.335	0.385
	CH <sub>3</sub> (N)	3.70	11.0	-0.055	-0.055
	H(Me)	2.30	100.0	0.070	0.070
Water	O	3.166	0.6502	-0.8476	
	H	0.0	0.0	0.4238	
DMSO P1	O	2.80	0.29922	-0.54	
	S	3.40	0.99741	0.54	
	CH <sub>3</sub>	3.80	1.2	0.0	
DMSO P2	O	2.80	0.29922	-0.459	
	S	3.40	0.99741	0.139	
	CH <sub>3</sub>	3.80	1.230	0.160	

simulation box. For the integration over time; we used the leap-frog algorithm with time step of  $10^{-15}$  s (1 fs) adopted from D. Fincham (CCP5 Information Quarterly, September 1981). In the starting configuration, the NMF and solvent molecules were located on a face-centred-cubic lattice with random orientations of solvent molecules. In order to find the appropriate box size for a desired pressure and temperature, we first carried out MD runs of 800–1000 ps at a constant pressure by employing the weak coupling scheme of Berendsen *et al.*<sup>42</sup>. During this initial phase of the simulations, the volume of the simulation box was allowed to fluctuate, and the average volume was determined at the end of the simulation was used to calculate the appropriate box size. Subsequently, the simulations were carried out in microcanonical ensemble where each system was equilibrated for 1.6–2.0 ns and the simulations were run for another 4–5 ns for the calculation of different structural and dynamical quantities.

### 3. Results and discussion

#### 3.1. Hydrogen bonding structure and properties

The effects of variation of pressure on the various interactions of *cis* and *trans*-NMF conformers with the surrounding aqueous/DMSO environment may be understood by analyzing radial distribution functions (RDFs) which are presented in Figs. 1–4.

The interactions amongst *cis* and *trans*-NMF molecules, in aqueous as well as in DMSO solution, have been represented by  $O_{NMF} \cdots H_{NMF}$  radial distribution functions in Fig. 1, for *cis-cis*, *cis-trans*, *trans-cis* and *trans-trans* combinations. It is noted that irrespective of composition and solvent, there are two distinct patterns of hydrogen bonding between the conformers of NMF depending on whether *cis/trans* NMF acts as the hydrogen bond donor. This behavior has also been noted in our recent study<sup>43</sup>, where we have explored the structural properties of liquid *cis/trans* NMF mixture with varying temperature and pressure. At  $X_{NMF} = 0.2$ , heteromeric hydrogen bonding ( $O_{trans}-H_{cis}$  in water/ $O_{cis}-H_{trans}$  in DMSO) is preferred over *cis-cis/trans-trans* hydrogen bonds, but as NMF concentrations increases, probability of  $O_{cis}-H_{cis}$  interactions is boosted in both water and DMSO solutions while  $O_{trans}-O_{trans}$  hydrogen bonds are not favorable which may be due to increase in number of *cis*-conformers in the solution. In aqueous solution ( $X_{NMF} = 0.2$ ), *trans-trans* and *cis-trans* correlations occur at first peak position of 2.48 Å while *trans-cis* correlations are greatly favorable and occur at shorter distances of 2.40 Å along with *cis-cis* NMF correlations occurring at 2.45 Å. As concentration of NMF changes in aqueous solution, all  $O_{NMF}-H_{NMF}$  correlations shift by 0.04 Å with higher interaction probability. In case of  $X_{NMF} = 0.2$  or 0.5 in DMSO, we note that first peak positions of all  $O_{NMF}-H_{NMF}$  correlations occur at shorter distances by around 0.08 Å than that of the corresponding RDFs in aqueous medium. So overall, from Fig. 1, it is clear that hydrogen bonding between NMF molecules is more favored in DMSO solution as is also seen from higher peak amplitude of correlations in DMSO solution than in aqueous solution. In binary NMF-DMSO mixtures, it has been proposed in literature that exchange of DMSO with NMF molecules can occur without much change to original NMF structure<sup>44</sup>. At higher concentrations of NMF, as well as at the highest pressure 350 MPa, NMF molecules in solution are brought closer and elevation in the probability of all  $O_{NMF} \cdots H_{NMF}$  interactions is noticed.

In Fig. 2,  $O_{SOLVENT}-H_{NMF}$  correlations have been depicted with variation of pressure and two different NMF compositions. In Fig. 2(a,b), we see that in the first solvation shell, probability of  $O_{WAT}-H_{N_{trans}}$  interactions is significantly higher with deeper minima than that of  $O_{WAT}-H_{N_{cis}}$  hydrogen bonds, which becomes more conspicuous at higher NMF ( $X_{NMF} = 0.5$ ) concentrations. For  $X_{NMF} = 0.2$ , it is observed that as pressure increases from 0.1 MPa–350 MPa, probability of

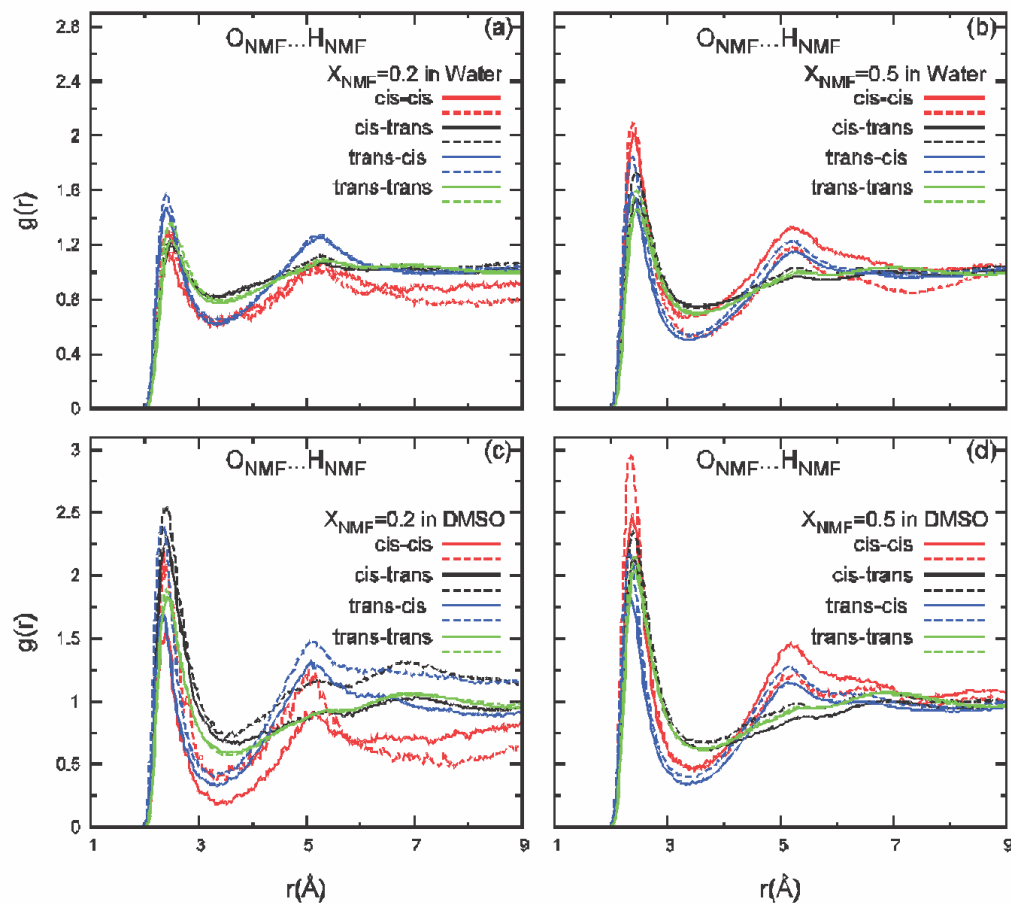
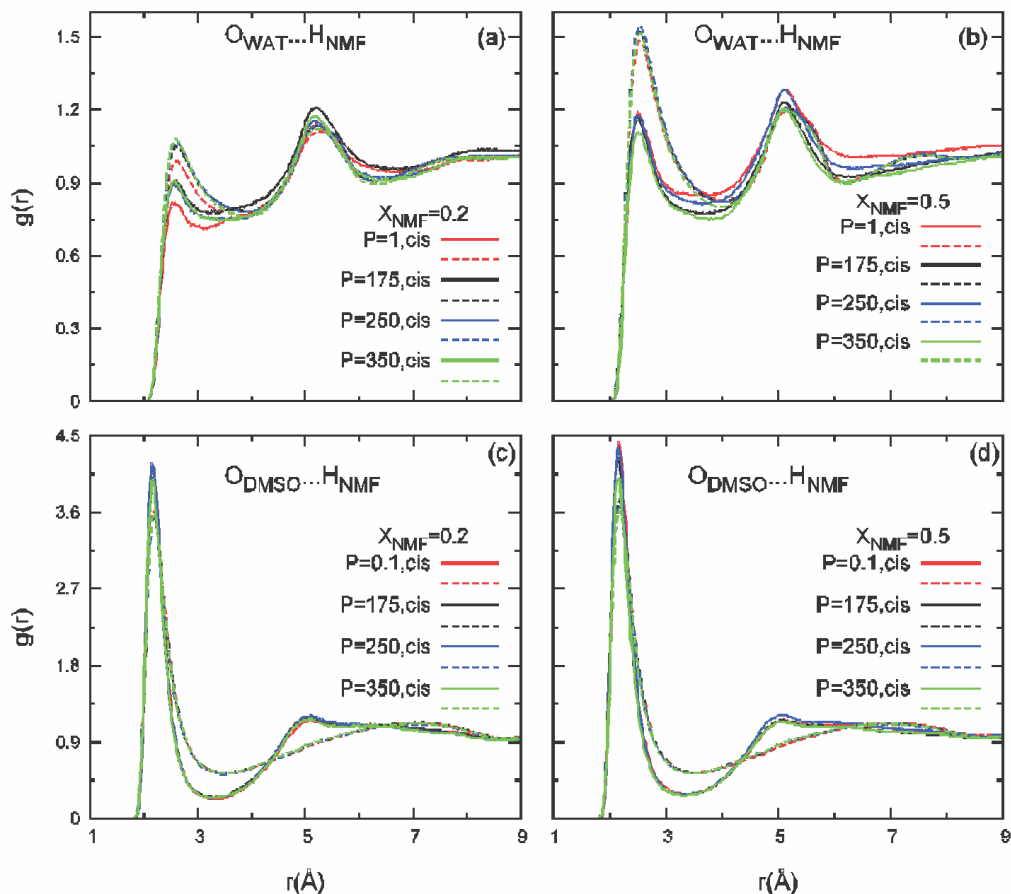


Fig. 1. Radial distribution functions between oxygen (*cis/trans*-NMF) – amide hydrogen (*cis/trans*-NMF) at (a)  $X_{\text{NMF}} = 0.2$  in water, (b)  $X_{\text{NMF}} = 0.5$  in water, (c)  $X_{\text{NMF}} = 0.2$  in DMSO and (d)  $X_{\text{NMF}} = 0.5$  in DMSO at 0.1 MPa and 350 MPa (shown by solid and dashed lines, respectively).

$O_{\text{WAT}}\text{-HN}_{\text{cis/trans}}$  hydrogen bonding increases initially and stays constant. At higher NMF concentrations,  $O_{\text{WAT}}\text{-H}_{\text{cis}}$  RDF peak heights decrease at the highest pressure i.e. 350 MPa while there is no change in  $O_{\text{WAT}}\text{-H}_{\text{trans}}$  correlations. Towards the second solvation shell at 5.17–5.25 Å, *cis*-NMF amide hydrogens prefer to be in the vicinity of water oxygens, particularly at intermediate concentrations. In a study of structural interactions between NMF-water molecules at varying mixture composition, it has been demonstrated by Hammami and Chebaane<sup>45</sup> that at higher water concentrations (as  $X_{\text{WAT}}$  increases from 0.5 to 0.75), the first peak of structure factor and  $g_{\text{HB}}^{\text{L}}$  decreases in amplitude which is similar to influence of pressure in typical hydrogen bonded liquids. The structure factor is often related to the molecular pair correlation functions and here we see that at  $X_{\text{NMF}} = 0.2$  (higher water fraction), the amplitude of correlations is lesser than that in lower water concentrations.

In DMSO solution (Fig. 2(c,d)), there is greater preference of amide hydrogen of *cis*-NMF for oxygen of DMSO as compared to *trans*-NMF which increases as mole fraction of NMF increases from  $X_{\text{NMF}} = 0.2$  to 0.5. Radial distribution functions between  $O_{\text{DMSO}}\text{-H}_{\text{cis}}$  sites have a prominent first peak occurring at 2.15 Å, with a well-defined second solvation shell at 5.05 Å whereas  $O_{\text{DMSO}}\text{-H}_{\text{trans}}$  RDFs are characterized by lesser peak heights, shallower minima leading to a broad second solvation shell around 7.2 Å. As pressure is increased, there is negligible change between  $O_{\text{DMSO}}\text{-H}_{\text{trans}}$  hydrogen bonding while a slight decrease in probability is seen for  $O_{\text{DMSO}}\text{-H}_{\text{cis}}$  correlations is observed. From Monte-Carlo studies by Cordeiro<sup>46</sup>, it has been predicted that  $O_{\text{NMF}}\text{-HN}_{\text{NMF}}$  hydrogen bonds can be naturally interchanged with  $O_{\text{DMSO}}\text{-HN}_{\text{NMF}}$  hydrogen bonds due to similar NMF-NMF and NMF-DMSO interaction energies. It has also been proposed that  $O_{\text{DMSO}}\text{-HN}_{\text{NMF}}$  hydrogen bonds may take over  $O_{\text{NMF}}\text{-$



**Fig. 2.** Radial distribution functions between oxygen(water) – hydrogen(NMF) at (a)  $X_{NMF} = 0.2$  in water and (b)  $X_{NMF} = 0.5$  in water and oxygen(DMSO)-hydrogen (NMF) at (c)  $X_{NMF} = 0.2$  in DMSO and (d)  $X_{NMF} = 0.5$  in DMSO with varying pressure (where *cis/trans*-NMF represented by solid/dashed lines, respectively).

$H_{NMF}$  hydrogen bonds at higher DMSO concentrations. In our work, we see that  $O_{DMSO} \cdots H_{trans-NMF}$  hydrogen bonds have no appreciable change as DMSO concentration is lowered ( $X_{NMF} = 0.5$ ), but  $O_{DMSO} \cdots H_{cis-NMF}$  hydrogen bonds have a better chance of formation at higher NMF concentrations.

Further, we compared P1 and P2 models of DMSO in Fig. 3, by considering behavior of  $O_{P1/P2DMSO} \cdots H_{cis/trans-NMF}$  RDFs. At low concentrations of NMF, there is not much difference in between the two models but as NMF concentration increases ( $X_{NMF} = 0.5$ ) at 0.1 MPa, *cis*-NMF amide hydrogen’s interaction with oxygen of DMSO is slightly higher for P2 model than for P1. However, at 350 MPa, the difference in interaction of oxygen of DMSO with amide hydrogen of *cis/trans*-NMF becomes negligible between P1/P2 models.

Some of the hydrogen bonds in solution were not appreciably affected by the application of pressure and the computed radial distribution functions have not been shown here. For instance, the effects of pressure on  $H_{WAT} \cdots O_{cis/trans-NMF}$  correlations (with first solvation shell occurring at 1.75 Å) are not much apparent, even at the highest pressure i.e. 350 MPa and the preferential difference between *cis/trans*-NMF oxygen for water hydrogen is also less significant at higher NMF concentration. Additionally, the effects of varying pressure do not appreciably perturb the local water-water interactions in both the concentrations taken here. At higher NMF concentrations, ordering of water structure is boosted due to localization of water molecules and more probability of finding water molecules as nearest neighbors.

The manifestation of pressure effects are more pronounced for hydrophobic interactions between methyl groups of DMSO as well as between methyl groups of DMSO and

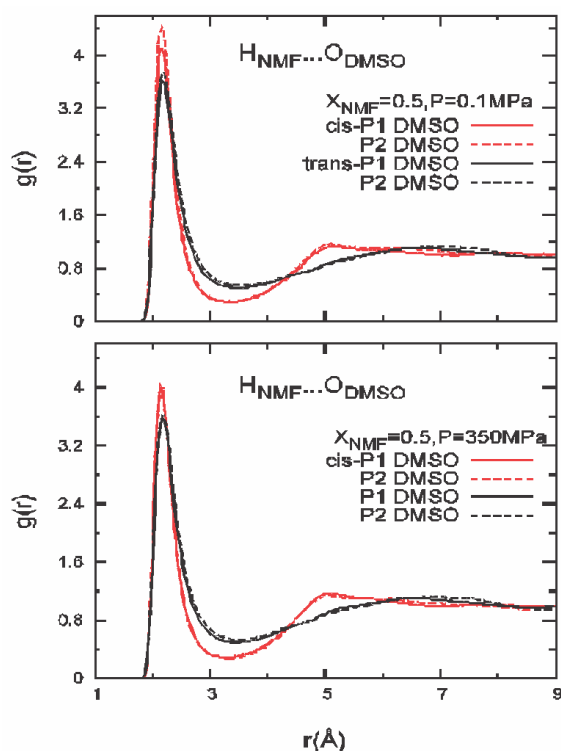


**Fig. 3.** Comparison of  $H_{cis/trans-NMF} \cdots O_{DMSO}$  radial distribution functions at  $X_{NMF} = 0.5$  for P1 and P2 models of DMSO at 0.1 and 350 MPa. The solid and dashed lines represent P1 and P2 models, respectively.

NMF molecules are illustrated in Fig. 4. In Fig. 4(a,b), the correlations between  $(CH_3)_{DMSO} \cdots (CH_3)_{DMSO}$  reach a peak positioned at 4.04 Å, which remains unchanged by variation in NMF concentration. For both  $X_{NMF} = 0.2$  and 0.5 solutions, the first minima is deepened with application of pressure, indicating reduced flexibility of interactions. The second solvation shell at 5.6 Å and the third broad shell spread over 8.0–9.2 Å remain unaffected by application of pressure. The methyl groups of DMSO may also interact with methyl groups attached to *cis/trans*-NMF molecules. The first peak maxima at 3.9 Å decreases in height as DMSO concentration in the solution decreases (i.e.  $X_{NMF} = 0.5$ ). In the first solvation shell, N-methyl group of *trans*-NMF interacts better with DMSO methyl group than its *cis* counterpart, and this tendency is seen to be enhanced with application of pressure. At lower pressures, *cis*-methyl groups are found to be in the vicinity of DMSO methyl groups as is seen from the  $H_3(C)_{cis-NMF} \cdots (CH_3)_{DMSO}$  second solvation shell at 5.64 Å while the  $H_3(C)_{trans-NMF} \cdots (CH_3)_{DMSO}$  RDF's second maxima

is found to be shifted from its *cis*-counterpart by 0.3 Å. As pressure is increased, the *cis*-methyl group has lower tendency to stay near DMSO methyl groups.

To calculate the hydrogen bond properties of hydrogen bonds between *cis*-water, *trans*-water and *water*-*water* hydrogen bonds, we use a set of *geometric criteria*<sup>47–50</sup>. For calculation of hydrogen bond properties, it is assumed that a hydrogen bond between two species exists, if the following distance and angular criteria are satisfied, i.e.  $R^{(OX)} < R_c^{(OX)}$ ,  $R^{(OH)} < R_c^{(OH)}$  and  $\theta < \theta_c$ . The distance cut-off values can also be obtained from the positions of first minimum of the corresponding radial distribution functions shown in Figs. 2 and 3. For oxygen of *cis*-NMF *trans*-NMF-hydrogen water hydrogen bond,  $R^{(OX)}$  and  $R^{(OH)}$  denote the oxygen (*water*)-nitrogen (*cis/trans*-NMF) and oxygen (*cis/trans*-NMF)-hydrogen (*water*) distances. Regarding the angular cut-off  $\theta_c$ , we have used the cut-off angle  $\theta_c = 45^\circ$  for the existence of NMF-water/DMSO hydrogen bonds in order to account for flexibility arising from thermal motion<sup>51</sup>.

The average number ( $n_{HB}$ ) and energies ( $E_{HB}$ ) of  $O_{NMF} \cdots H_{WAT}$ ,  $H_{NMF} \cdots O_{WAT/DMSO}$  intermolecular hydrogen-bonds between different combination of *cis*- and *trans*-NMF have been calculated. When a single *trans*-NMF molecule is present in water/DMSO,  $O_{trans-NMF} \cdots H_{WAT}$  is energetically stable and with respect to pressure, the average hydrogen bond number and energy varies from 1.98 and –20.469 kJ/mol respectively at 0.1 MPa to 2.03 and –19.67 kJ/mol respectively at 350 MPa. In DMSO solution, there is not much difference in the range of average hydrogen bond number (0.92–0.93) and energy (–22.226 to –22.470 kJ/mol), upon application of higher pressure. It may be noted that these hydrogen bonds are more stable than those in aqueous solution, although there is negligible effect of pressure in DMSO solutions.

We see that in aqueous solutions, there are two kinds of hydrogen bonds,  $H_{WAT} \cdots O_{trans/cis-NMF}$  and  $O_{WAT} \cdots H_{trans/cis-NMF}$ . The average hydrogen bond number and energy of the  $H_{WAT} \cdots O_{trans/cis-NMF}$  hydrogen bonds have more average number (~0.84–1.52) as well as energy (–21–22 kJ/mol) than that of the  $O_{WAT} \cdots H_{trans/cis-NMF}$  hydrogen bonds which have lesser number (~0.35–0.56) and stability (with  $E_{HB}$  in the range –7 to –10 kJ/mol). Both these hydrogen bonds show increase in stability as NMF concentration in the solution increases although their average number decreases as

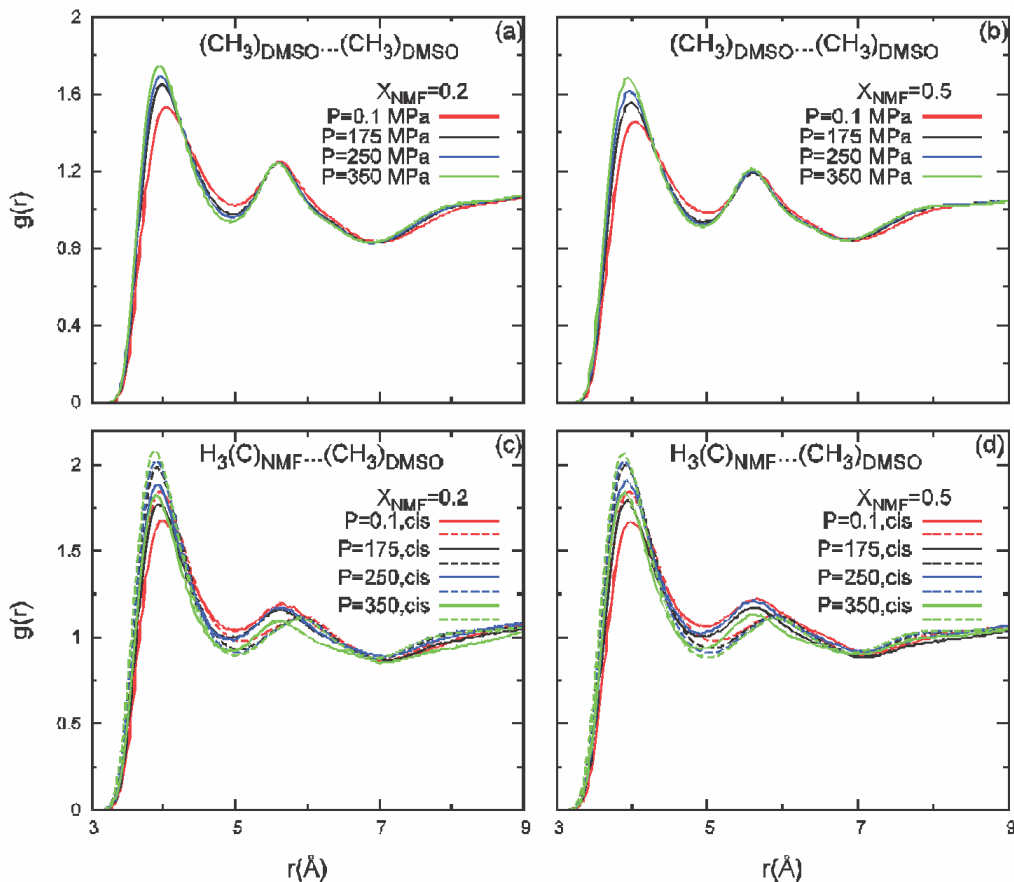


**Fig. 4.** Radial distribution functions between  $(CH_3)_{DMSO} \cdots (CH_3)_{DMSO}$  at (a)  $X_{NMF} = 0.2$  and (b)  $X_{NMF} = 0.5$  in DMSO and  $H_3(C)_{NMF} \cdots (CH_3)_{DMSO}$  at (c)  $X_{NMF} = 0.2$  and (d)  $X_{NMF} = 0.5$  in DMSO solution with varying pressure (where *cis/trans*-NMF represented by solid/dashed lines, respectively).

probability of NMF-NMF hydrogen bonds increases. Upon application of pressure, there is not much appreciable variation of hydrogen bond number and energy ( $\Delta E_{HB} = 0.1\text{--}0.2$  kJ/mol) for  $H_{WAT} \cdots O_{trans/cis-NMF}$  hydrogen bonds. The energetically weaker  $O_{WAT} \cdots HN_{cis/trans-NMF}$  hydrogen bonds show decrease in hydrogen bond stability upon application of pressure due to distortion of hydrogen bond network but slight increase in hydrogen bond number is noted which may be due to compression effects. Even at higher NMF concentrations, we observe that with increasing pressure, the stability of hydrogen bonds is decreasing as the  $E_{HB}$  for  $O_{WAT} \cdots HN_{cis}$  hydrogen bonds changes from  $-10.03$  kJ/mol to  $-9.48$  kJ/mol while that for  $O_{WAT} \cdots HN_{trans}$  hydrogen bonds decreases from  $-8.41$  kJ/mol to  $-7.69$  kJ/mol.

As solution changes to aprotic medium, we observe that in general, the average hydrogen bond number and stability

of  $O_{DMSO} \cdots HN_{cis/trans-NMF}$  hydrogen bonds slightly decreases at higher pressures. For example, at higher NMF concentrations, as we increase the pressure upto 350 MPa, the average number of  $O_{DMSO} \cdots HN_{trans-NMF}$  remains constant at 0.55 while the energy slightly changes from  $-22.55$  kJ/mol to  $-22.34$  kJ/mol. There is a negligible difference in the average number of hydrogen bonds ( $H_{cis/trans-NMF} \cdots O_{DMSO}$ ) in between the two models of DMSO (P1 and P2), while the  $H_{cis/trans-NMF} \cdots O_{P1-DMSO}$  hydrogen bond energy is less than that of  $H_{cis/trans-NMF} \cdots O_{P2-DMSO}$  hydrogen bond ( $\Delta E_{HB} = -0.5$  to  $-1.6$  kJ/mol).

### 3.2. Self-diffusion coefficients and orientational relaxation times

The translational self-diffusion coefficient  $D_i$  of species  $i$  is related to the time integral of the velocity-velocity autocorrelation function (VAF) by

$$D_i = \frac{k_B T}{m_i} \int_0^\infty C_v(t) dt, \quad (2)$$

where  $k_B$  is the Boltzmann's constant and  $m_i$  is the mass of species  $i$  and  $C_v(t)$  is the velocity-velocity time correlation function,  $C_v(t)$ , defined by

$$C_v(t) = \frac{\langle \mathbf{v}_i(t) \cdot \mathbf{v}_i(0) \rangle}{\langle \mathbf{v}_i(0) \cdot \mathbf{v}_i(0) \rangle}, \quad (3)$$

where  $\mathbf{v}_i(t)$  is the velocity of the species  $i$  at time  $t$ <sup>52</sup> and the average is carried out over all the species in the system and over the initial time. The  $C_v(t)$  plot for *cis/trans* NMF molecules in both the solutions at varying pressure have been depicted in Fig. 5.

The translational self-diffusion coefficient can also be calculated from the long-time limit of the mean-square displacement (MSD)

$$D_i = \lim_{t \rightarrow \infty} \frac{\langle |\mathbf{r}(t) - \mathbf{r}(0)|^2 \rangle}{6t}, \quad (4)$$

where  $\mathbf{r}(t)$  is the position of a species  $i$  at time  $t$ , by a least-square fit of the long-time region of MSD as obtained from simulations. The diffusion coefficients calculated using these two routes have been found to be quite close to each other and we have taken the average of the values obtained from these two routes for a given type of species and plotted these values in Fig. 6(a,b).

It is observed that translational motion becomes sluggish as solvent concentration (water/DMSO) decreases and pressure increases. At 0.1 MPa, the difference in diffusion values between *cis* and *trans*-NMF molecules are more visible at higher NMF concentrations. At pressures of 250 MPa and 350 MPa, there is a significant decrease in diffusion rates at all compositions but at the same time, disparity between diffusion rates of *cis* and *trans*-NMF molecules becomes negligible, in either water/DMSO solution. From literature, it has been seen that *trans*-NMF conformers can form long linear molecular chains while *cis*-NMF molecules are more likely to form cyclic ring-like structures. On increasing pressure, any caging effects in *cis*-molecules are eroded by difficulty in maintaining ring closure of *cis*-NMF molecules and thus *cis*-NMF molecules do not exhibit much difference in self-diffusion coefficients with respect to its *trans*-NMF con-

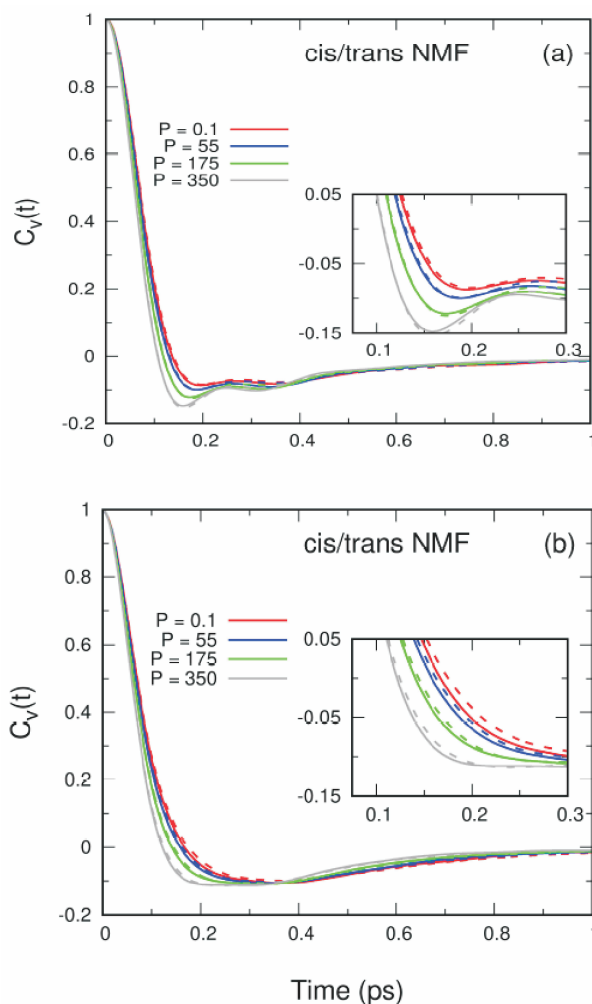


**Fig. 5.** The decay of velocity-velocity autocorrelation functions at  $X_{\text{NMF}} = 0.2$  in (a) DMSO and (b) water solution with varying pressure (where *cis/trans*-NMF represented by solid/dashed lines, respectively).

former at higher pressures. This can be seen from decay of velocity-velocity autocorrelation functions in both DMSO and water solutions in Fig. 5 where the differences in caging (more for *cis*-NMF molecules than *trans*-NMF at lower pressure) are not that prominent at higher pressures. The differential caging effects for *cis/trans*-NMF and their variation with pressure has been noted in more detail in our recent study for neat NMF<sup>43</sup>, where difference in self-diffusion coefficients in *cis* and *trans*-NMF has been observed to be reduced at higher pressures. In DMSO, we note difference in the diffusion behaviour of *cis* and *trans*-NMF that decreases with pres-



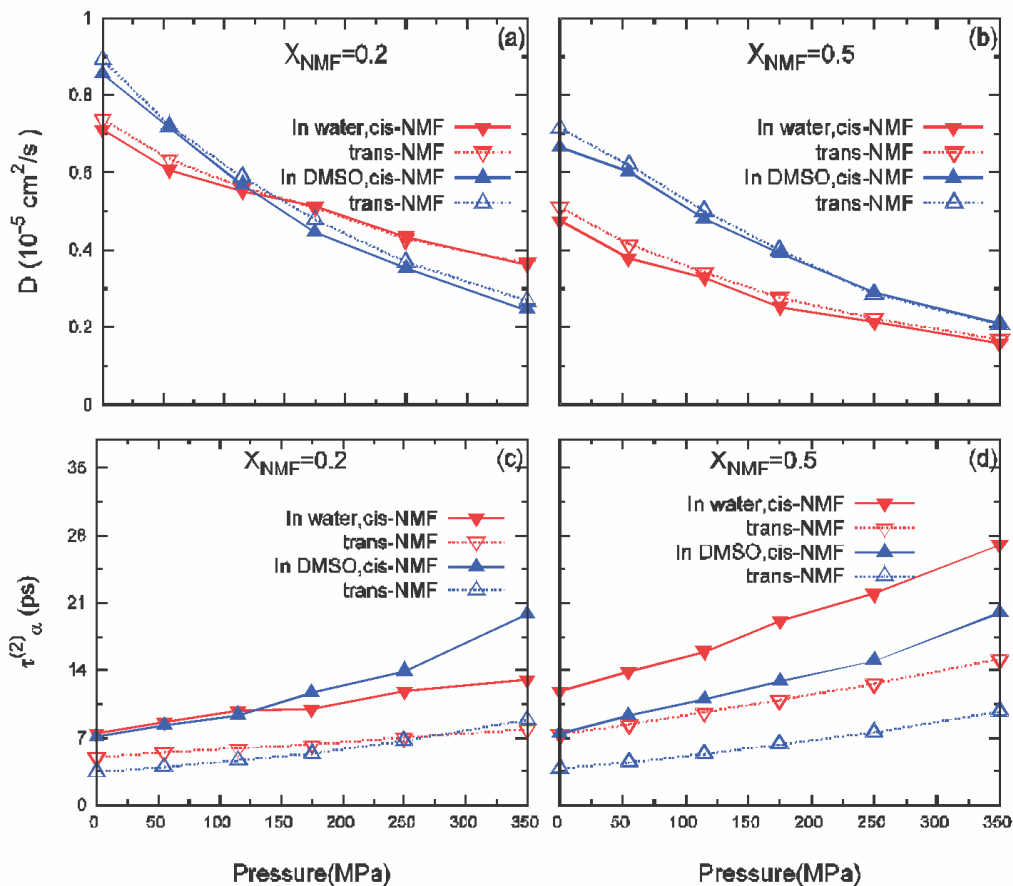


Fig. 6. The self-diffusion coefficients of *cis* and *trans*-NMF at varying pressures for water/DMSO solution composition of (a)  $X_{\text{NMF}} = 0.2$  and (b)  $X_{\text{NMF}} = 0.5$  and dipole vector orientational correlation times of *cis* and *trans*-NMF for solution composition of (c)  $X_{\text{NMF}} = 0.2$  and (d)  $X_{\text{NMF}} = 0.5$ .

sure and it may be due to the fact that the donating ability of hydrogen bond of *cis*-NMF is less stable ( $E_{\text{HB}}$  of  $\text{O}_{\text{DMSO}} \cdots \text{HN}_{\text{cis}}$  hydrogen bond is in the range  $-20$  to  $-21$  kJ/mol) in comparison of that of the *trans*-NMF (where  $E_{\text{HB}}$  of  $\text{O}_{\text{DMSO}} \cdots \text{HN}_{\text{trans}}$  hydrogen bond is in  $\sim -22$  kJ/mol), leading to difference in hydrogen bonding with the aprotic environment. We have also calculated the diffusion coefficients of *cis* and *trans*-NMF using the P1 model of DMSO and we see that though trends with pressure remain similar, the values are appreciably less than that of those obtained with P2 model of DMSO. For example, at 0.1 MPa, the values of self-diffusion coefficients for *cis* and *trans*-NMF in DMSO (P2) solution are  $D(\times 10^{-5} \text{ cm}^2/\text{s}) = 0.858$  and  $0.892$  whereas in DMSO (P1) solution, the values are reduced to  $0.68$  and  $0.72$  for *cis/trans*-NMF respectively. The motion of both *cis* and *trans*-NMF molecules is seen to be more retarded in aqueous solutions as composition of NMF increases which may be due

to variable formation of *cis/trans*-NMF-water hydrogen bonds in solution. It is seen that there is negligible difference of probability of hydrogen bonding and stability of hydrogen bond acceptance of both *cis/trans*-NMF for water molecules i.e. for  $\text{H}_{\text{WAT}} \cdots \text{O}_{\text{cis/trans}}$  hydrogen bonds, the average hydrogen bond energies are similar for both concentrations i.e. at  $X_{\text{NMF}} = 0.2$  ( $E_{\text{HB}} \sim -21$  kJ/mol) and  $0.5$  ( $E_{\text{HB}} \sim -22$  kJ/mol). However, change in stability of donating *trans*-NMF hydrogen bond is more compared to *cis*-NMF hydrogen bond. For example at  $X_{\text{NMF}} = 0.5$  and  $0.1$  MPa,  $E_{\text{HB}}$  of  $\text{O}_{\text{WAT}} \cdots \text{H}_{\text{N}_{\text{cis}}}$  hydrogen bond =  $-10.029$  kJ/mol and  $E_{\text{HB}}$  of  $\text{O}_{\text{WAT}} \cdots \text{HN}_{\text{trans}}$  hydrogen bond =  $-8.405$  kJ/mol. We have seen from Fig. 2 that as concentration of NMF increases, the probability of hydrogen bonding of water oxygen with *cis/trans*-NMF increases and the difference between  $\text{O}_{\text{WAT}} \cdots \text{H}_{\text{cis}}$  and  $\text{O}_{\text{WAT}} \cdots \text{H}_{\text{trans}}$  correlations becomes more conspicuous. So difference in *cis/trans*

diffusion behaviour is prominent at  $X_{\text{NMF}} = 0.5$  concentration in aqueous solution.

Experimental studies by Easteal and Woolf and at 298 K show that self-diffusion values for NMF (neat) change from  $D$  ( $10^{-5} \text{ cm}^2/\text{s}$ ) =  $0.84 \times 10^{-5} \text{ cm}^2/\text{s}$  to  $0.32 \times 10^{-5} \text{ cm}^2/\text{s}$  as pressure increases from 0.1 MPa to 273.2 MPa. In an earlier study, Lüdemann and co-workers<sup>53</sup> had evaluated diffusion values in neat NMF using pulsed gradient spin echo method, at similar pressures as in our calculations. Chen *et al.*<sup>54</sup> compared diffusion coefficients of *cis* and *trans*-NMF conformers in liquid NMF and demonstrated 17% slowdown of *cis*-NMF relative to *trans*-NMF below  $\sim 270$  K while the difference comes down to around 8.5% at 298 K and 0.1 MPa. Skarmoutsos and Samios<sup>55</sup> have predicted the difference between *cis* and *trans*-NMF diffusion coefficients to be 5.5% in neat NMF. Spin-echo NMR experiments by Fratiello<sup>56</sup> predicted the self-diffusion coefficients of NMF molecules in  $\text{D}_2\text{O}$  at 313 K for various compositions. At 25% and 50% volume percent of NMF in  $\text{D}_2\text{O}$ , the self-diffusion coefficients were calculated to be 0.95 and 0.75 ( $\times 10^{-5} \text{ cm}^2/\text{s}$ ) respectively. Errors in the self-diffusion coefficients of NMF are possible due to proton exchanges between amide and water for which contribution of HDO to the diffusion data have not been estimated.

The orientational motion of solvent molecules is analyzed by calculating the orientational time correlation function,  $C_l^\alpha(t)$ , defined by

$$C_l^\alpha(t) = \frac{\langle P_l[\mathbf{e}^\alpha(t) \cdot \mathbf{e}^\alpha(0)] \rangle}{\langle P_l[\mathbf{e}^\alpha(0) \cdot \mathbf{e}^\alpha(0)] \rangle}, \quad (5)$$

where  $P_l$  is the Legendre polynomial of rank  $l$  and  $\mathbf{e}^\alpha$  is the unit vector which points along the  $\alpha$ -axis in the molecular frame. In this work, we have calculated the time dependence of  $C_l^\alpha(t)$  for  $l = 2$ , and for dipole vector of *cis* and *trans*-NMF.

The orientational correlation time  $\tau_l^\alpha$ , defined as the time integral of the orientational correlation function

$$\tau_l^\alpha = \int_0^\infty dt C_l^\alpha(t) \quad (6)$$

were obtained by explicit integration of the data of  $C_l^\alpha(t)$  from simulations up to 25 ps for NMF till the values are properly converged and these values have been presented in Fig. 6(c,d).

At 0.1 MPa, there is insignificant change in orientational relaxation times of *cis/trans*-NMF dipole vectors upon increase in concentration from  $X_{\text{NMF}} = 0.2$  to  $X_{\text{NMF}} = 0.5$  in DMSO solution compared to that in water where the relaxation times of both *cis* and *trans* isomers increase upon increase in NMF concentration. At  $X_{\text{NMF}} = 0.2$ , it is observed that at higher pressures, the NMF dipole vector reorients more slowly in DMSO solution compared to that in aqueous medium specially for *cis*-NMF dipole orientation (the affinity of oxygen of DMSO for *cis*-NMF has been discussed in earlier section). It has been established from earlier studies that NMF-DMSO mixture at various compositions have strong dipole-dipole correlations leading to a well-ordered structure of the resulting solution and this may be the result of slower rotation of NMF isomers in DMSO solution<sup>44</sup>. It is interesting to see that as the concentration of NMF increases in DMSO as well as in water solutions, slowdown in orientational motion occurs and the difference in orientational motion between *cis* and *trans*-NMF dipole rotations is more noticeable in aqueous medium at higher pressures. For example, at  $X_{\text{NMF}} = 0.5$  in aqueous solution, *cis*-NMF takes 9.83 ps at 0.1 MPa to 27.01 ps at 350 MPa for reorienting its dipole vector while for *trans*-NMF, the reorientation times are 7.39 ps to 15.14 ps at 0.1 MPa and 350 MPa respectively. There is not much variation in orientational relaxation times of *cis/trans*-NMF at higher NMF concentrations in case of DMSO solution. Our calculated dipole vector orientational relaxation times are presented in Fig. 6(c,d). From NMR experiments, Weingartner and co-workers<sup>57</sup> have calculated reorientational correlation times of water and NMF molecules as a function of various mole fractions and though not directly comparable, our results show a similar trend to the experimental results that is as concentration of NMF increases, the difference between NMF and water reorientational correlation times increases with overall slower rotation of NMF relative to water molecules.

We also calculated the translational and rotational dynamics of a single *trans*-NMF molecule in water and in DMSO solution. The self-diffusion coefficients,  $D$  ( $\times 10^{-5} \text{ cm}^2/\text{s}$ ), for *trans*-NMF in aqueous solution changed from 1.06 to 0.87 upon variation of pressure from 0.1 MPa–350 MPa, while in DMSO solution, the values change from 0.71 to 0.36 at higher pressures.

### 3.3. Hydrogen bond lifetimes

To calculate the hydrogen bond dynamics of amide-water, water-water, we define two hydrogen bond population variables  $h(t)$  and  $H(t)$ , where  $h(t)$  is unity when a particular NMF-water, NMF-DMSO or water-water pair is hydrogen bonded at time  $t$  according to the adopted hydrogen-bond definition discussed above and zero otherwise. Whereas,  $H(t) = 1$  if the NMF-water and water-water pair remain continuously hydrogen bonded from  $t = 0$  to time  $t$ , and it is zero otherwise.

To study the breaking dynamics of hydrogen bonds, we calculate the continuous hydrogen-bond time correlation function, which is defined as<sup>58–61</sup>

$$S_{\text{HB}}(t) = \langle h(0) H(t) \rangle / \langle h(0)^2 \rangle \quad (7)$$

where  $\langle \dots \rangle$  denotes an average over all *cis/trans*-NMF-water/DMSO and water-water pairs. Clearly,  $S_{\text{HB}}(t)$  describes the probability that an initially hydrogen bonded amide-water and water-water pair remain bonded at all times up to  $t$ . The associated integrated relaxation time  $\tau_{\text{HB}}$  can be interpreted as the average lifetime of a hydrogen bond. In case of these hydrogen-bonds, the decay of time correlation function is calculated up to 25 ps depending on the proper convergence of this function.

We have calculated the hydrogen bond lifetimes of the dominant hydrogen bonds in each solution i.e.  $\text{H}_{\text{cis/trans-NMF}}\text{-O}_{\text{DMSO}}$  in DMSO solution and  $\text{O}_{\text{cis/trans-NMF}}\text{-H}_{\text{WAT}}$  in aqueous mixture and they are presented in Tables 2–4 for  $X_{\text{NMF}} = 0.04, 0.2$  and  $0.5$  solution compositions. Since  $\text{HN}_{\text{cis/trans-NMF}}$  hydrogen bonds are of higher energy ( $-7.4$  to  $-10.03$  kJ/mol) and hence their lifetime has not been shown here.

All hydrogen bond lifetimes increase with higher pres-

**Table 2.** Average hydrogen bond lifetime of  $\text{O}_{\text{trans-NMF}}\text{-H}_{\text{WAT}}$  hydrogen bond in aqueous solution and  $\text{O}_{\text{DMSO}}\text{-H}_{\text{cis-NMF}}$  hydrogen bond in DMSO solution where  $X_{\text{NMF}} = 0.04$  (or a single *trans*-NMF in 499 solvent molecules)

P (MPa)	$\tau_{\text{HB}}$ (ps) $X_{\text{NMF}} = 0.04$	
	$\text{O}_{\text{trans}}\text{-H}_{\text{W}}$	$\text{O}_{\text{DMSO}}\text{-H}_{\text{cis}}$
0.1	1.03	0.58
55	1.10	0.69
115	1.10	0.59
175	1.03	0.72
250	0.91	0.84
350	0.94	0.85

sure since compressions in available volume bring the NMF-water/DMSO sites closer and this can lead to longer association times. It is observed that in aqueous mixture, as concentration of NMF increases, lifetime of  $\text{O}_{\text{cis/trans-NMF}}\text{-H}_{\text{WAT}}$  hydrogen bonds increases due to better stability of hydrogen bonds as is and this trend is particularly conspicuous at higher pressures. It is well known from literature that *cis*-NMF molecules prefer to form flexible ring-like hydrogen bonded networks with other *cis* molecules or with solvent molecules<sup>62</sup> (for e.g. three-centered  $\text{H}_{\text{WAT}}\text{-O}_{\text{cis}}$  hydrogen bonds). At intermediate pressures, in the water-rich solution ( $X_{\text{NMF}} = 0.2$ ), it is possible that probability of other water molecules drifting near the *cis*-water hydrogen bonded rings increases. So, the hydrogen bonding probability of the water molecules that participates in *cis*-water hydrogen bonding with that of the vicinal water molecule may increase, which can hinder the lifetime of *cis*-water hydrogen bonded system. But overall at much higher pressures, lifetime increases due to excluded volume effects that do not permit much proximity between solvent molecules.

**Table 3.** Average hydrogen bond lifetime of  $\text{O}_{\text{cis/trans-NMF}}\text{-H}_{\text{WAT}}$  hydrogen bond in aqueous solution and  $\text{O}_{\text{DMSO}}\text{-H}_{\text{cis/trans-NMF}}$  hydrogen bond in DMSO solution where  $X_{\text{NMF}} = 0.2$  in both solutions. The values for P1 model of DMSO at some pressures are given in brackets

P (MPa)	$\tau_{\text{HB}}$ (ps) $X_{\text{NMF}} = 0.2$				
	$\text{O}_{\text{cis}}\text{-H}_{\text{W}}$	$\text{O}_{\text{trans}}\text{-H}_{\text{W}}$	$\text{O}_{\text{DMSO}}\text{-H}_{\text{cis}}$ P2 (P1)	$\text{O}_{\text{DMSO}}\text{-H}_{\text{trans}}$ P2 (P1)	$\text{O}_{\text{WAT}}\text{-H}_{\text{WAT}}$
0.1	2.09	2.31	1.35 (1.36)	0.67 (0.69)	2.40
55	2.13	2.45	1.36	0.68	2.44
115	2.12	2.44	1.46 (1.37)	0.69 (0.73)	2.46
175	1.96	2.45	1.46	0.71	2.61
250	2.22	2.51	1.47 (1.46)	0.72 (0.72)	2.59
350	2.15	2.58	1.54 (1.44)	0.76 (0.80)	2.64

**Table 4.** Average hydrogen bond lifetime of  $O_{cis/trans-NMF}\cdots H_{WAT}$  hydrogen bond in aqueous solution and  $O_{DMSO}\cdots H_{cis/trans-NMF}$  hydrogen bond in DMSO solution where  $X_{NMF} = 0.5$  in both solutions

P (MPa)	$\tau_{HB}$ (ps) $X_{NMF} = 0.5$				
	$O_{cis}\cdots H_w$	$O_{trans}\cdots H_w$	$O_{DMSO}\cdots H_{cis}$ P2 (P1)	$O_{DMSO}\cdots H_{trans}$ P2 (P1)	$O_{WAT}\cdots H_{WAT}$
0.1	3.72	4.10	1.21 (1.23)	0.67 (0.69)	5.09
55	3.80	4.48	1.25	0.68	5.44
115	4.30	4.59	1.27 (1.37)	0.70 (0.74)	5.70
175	4.56	4.60	1.29	0.71	6.30
250	4.13	4.95	1.27 (1.36)	0.72 (0.78)	6.13
350	4.56	5.00	1.36 (1.33)	0.73 (0.82)	6.52

As compared to  $O_{cis}\cdots H_{WAT}$  hydrogen bonds,  $O_{trans}\cdots H_{WAT}$  hydrogen bonds stay associated for slightly longer periods. In particular, it has been seen that  $O_{trans}\cdots H_{WAT}/DMSO$  hydrogen bond lifetimes show only little variations with increase of pressure and this has also been seen from neutron scattering experiments conducted by Nasr and co-workers<sup>63</sup> of deuterated liquid NMF at pressures ranging from 1–4 kbar. It has been noted that the hydrogen bonding is not appreciably changed by change in pressure and that slight changes may be attributed to density variations that lead to changes in distances between NMF hydrogen bonded chains. As concentration of NMF increases,  $HN_{NMF}\cdots O_{DMSO}$  hydrogen bond lifetimes decrease since there is a chance of NMF-NMF interactions dominating in the solution. An increase in hydrogen bond lifetime of  $O_{DMSO}\cdots H_{trans}$  is seen when the P1 model of DMSO is chosen as is seen from Tables 3 and 4. As seen from the RDFs in Fig. 2, as *cis*-NMF hydrogen is preferred by DMSO oxygen, the lifetimes of  $O_{DMSO}\cdots H_{cis}$  hydrogen bonds are higher than that of those involving *trans*-NMF hydrogen. Water-water hydrogen bond lifetimes decrease as concentration of NMF increases in solution.

#### 4. Conclusions

We have carried out a series of molecular dynamics simulations involving mixture of *cis* and *trans*-NMF molecules in protic/aprotic solvent medium at pressures varying from 0.1 MPa to 350 MPa at  $X_{NMF} = 0.2$  and 0.5 in water/DMSO solution. We have also taken a single *trans*-NMF molecule in water/DMSO solvent to compare some of the hydrogen bonding attributes. It is observed that *trans*-NMF molecules prefer to donate their hydrogen bonds to water oxygen sites and this is encouraged at higher NMF concentrations irre-

spective of pressure while *cis*-NMF molecules prefer hydrogen sites of water molecules. NMF-NMF interactions are boosted in DMSO solutions relative to that in aqueous medium. At higher pressures, *cis*-molecules come closer due to compressions in available volume leading to boost in  $O_{cis}\cdots H_{cis}$  correlations at both  $X_{NMF} = 0.2$  and 0.5 in water/DMSO solutions. It is observed that there is higher probability of *cis*-NMF molecules preferring to hydrogen bond with oxygen of DMSO while N-methyl groups of *trans*-NMF molecules prefer to interact via hydrophobic contacts to DMSO methyl groups, which is encouraged at increasing pressure. Comparison of P1 and P2 models of DMSO with respect to  $O_{DMSO}\cdots HN_{NMF}$  is noticeable only at  $X_{NMF} = 0.5$  where *cis*-NMF molecules exhibit slight preference for P2 model at 0.1 MPa but at higher pressures, the P1 and P2 models behave in similar fashion. The average hydrogen bond number, energy, lifetime as well as diffusion coefficients for P1 model of DMSO have also been calculated. Overall, intermediate pressures can encourage more probability of hydrogen bonding; however, such forced proximity leads to strain in hydrogen bond network leading to lesser hydrogen bond stabilities at higher pressures.

The difference between *cis* and *trans*-NMF self-diffusion coefficients is apparent at lower pressure ranges and at higher NMF concentrations. Both *cis* and *trans*-NMF molecules can hydrogen bond to water molecules at the amide hydrogen and carbonyl oxygen sites respectively and this may lead to sluggish translational motion in aqueous solutions which is further slowed down at higher pressures. A more ordered structure in DMSO solution due to strong dipole-dipole correlation between NMF and DMSO molecules results in longer orientational relaxation times as it is possible that methyl-

groups of NMF rotate more slowly in DMSO solutions giving rise to longer relaxation times. The disparity between *cis* and *trans*-NMF dipole rotations become more apparent in aqueous medium at higher pressures. The higher lifetimes of  $O_{\text{DMSO}}-H_{\text{cis}}$  hydrogen bonds are responsible for longer dipole relaxation times of *cis*-NMF in DMSO solutions. The variation in hydrogen bond lifetimes upon pressure and composition changes are more dramatic in case of aqueous than DMSO solutions since NMF-DMSO solutions are associated through hydrophobic as well as hydrogen bonding interactions and present stronger resistance to effects of pressure. However, overall, with variation of pressure only subtle changes in hydrogen bond lifetimes have been noticed.

In light of all these arguments, we conclude that pressure variably influences various structural and dynamical properties of *cis* and *trans*-NMF molecules in their aqueous/DMSO solution mixture. The degree to which variation of pressure induces alterations in the structure, stability, dynamics and motion of the molecules in water or DMSO depends on an interplay of excluded volume effects, compression effects, rigidity of the hydrogen bonding framework as well as different hydrogen bonding patterns preferred by *cis/trans*-NMF molecules that changes with surrounding protic/aprotic environment.

We are presently trying to extend these composition dependent studies in water/DMSO solutions by increasing overall NMF concentrations. Apart from maintaining the experimentally established mole fraction of 0.94 for *trans* isomer in *cis/trans*-NMF mixtures in such simulations, we hope to conduct simulations involving equal proportions of *cis* and *trans*-NMF isomers in the mixture to gain an understanding of hydrogen bond properties and diffusivity. The proportion of *trans* isomers in *cis/trans*-NMF mixture could change in some exceptional cases depending on temperature and solvent conditions. For instance, in an apolar solvent like  $\text{CDCl}_3$ , the abundance of *trans* isomer is around 88.8% (at 293 K) in comparison to that in water and methanol where it is around 94%. Theoretical studies of increased proportions of *cis* isomers could probably provide an impetus to experimental research in this direction. Further, considering the diverse interactions of *cis* and *trans*-conformers of NMF with their surrounding aqueous/non-aqueous environment, it is exciting to examine their behaviour in varying compositions of water-DMSO mixture and we are also presently working in this direction.

## Acknowledgement

Authors are grateful to the Council of Scientific and Industrial Research (CSIR), Government of India for SRF-fellowship and also to the Indian Institute of Technology, Bhubaneswar for all kinds of support to execute the Project.

## References

1. B. B. Boonyaratanakornkit, C. B. Park and D. S. Clark, *Biochim. Biophys. Acta BBA-Protein Struct. Mol. Enzymol.*, 2002, **1595**, 235.
2. M. S. Weiss, A. Jabs and R. Hilgenfeld, *Nat. Struct. Mol. Biol.*, 1998, **5**, 676.
3. A. B. Brauer, G. J. Domingo, R. M. Cooke, S. J. Matthews and R. J. Leatherbarrow, *Biochemistry (Mosc.)*, 2002, **41**, 10608.
4. M. S. Weiss, H. J. Metzner and R. Hilgenfeld, *FEBS Lett.*, 1998, **423**, 291.
5. D. Pal and P. Chakrabarti, *J. Mol. Biol.*, 1999, **294**, 271.
6. D. E. Stewart, A. Sarkar and J. E. Wampler, *J. Mol. Biol.*, 1990, **214**, 253.
7. L. A. LaPlanche and M. T. Rogers, *J. Am. Chem. Soc.*, 1964, **86**, 337.
8. Y. K. Kang, *J. Mol. Struct. THEOCHEM*, 2001, **546**, 183.
9. S. Ataka, H. Takeuchi and M. Tasumi, *J. Mol. Struct.*, 1984, **113**, 147.
10. F. Hammami, M. Bahri, S. Nasr, N. Jaidane, M. Oummezzine and R. Cortes, *J. Chem. Phys.*, 2003, **119**, 4419.
11. I. Suzuki, *Bull. Chem. Soc. Jpn.*, 1962, **35**, 540.
12. T. Miyazawa, T. Shimanouchi and S. Mizushima, *J. Chem. Phys.*, 1956, **24**, 408.
13. I. Skarmoutsos and J. Samios, *Chem. Phys. Lett.*, 2004, **384**, 108.
14. A. J. Easteal and L. A. Woolf, *J. Chem. Soc., Faraday Trans. 1*, 1985, **81**, 2821.
15. L. Chen, T. Gross, H.-D. Lüdemann, H. Krienke and R. Fischer, *Naturwissenschaften*, 2000, **87**, 225.
16. L. Chen, T. Gross and H.-D. Lüdemann, *Z. Für Phys. Chem.*, 2000, **214**, 239.
17. E. N. Gate, M. D. Threadgill, M. F. Stevens, D. Chubb, L. M. Vickers, S. P. Langdon, J. A. Hickman and A. Gescher, *J. Med. Chem.*, 1986, **29**, 1046.
18. M. Iwakawat, P. J. Tofilon, N. Hunter, L. C. Stephens and L. Milas, *Clin. Exp. Metastasis*, 1987, **5**, 289.
19. A. Fratiello, *Mol. Phys.*, 1964, **7**, 565.
20. A. Fratiello, R. E. Lee, D. P. Miller and V. M. Nishida, *Mol. Phys.*, 1967, **13**, 349.
21. S. Akhtar, A. N. M. Omar Faruk and M. A. Saleh, *Phys. Chem. Liq.*, 2001, **39**, 383.
22. M. N. Islam, M. A. Ali, M. Monirul Islam and M. K. Nahar, *Phys. Chem. Liq.*, 2003, **41**, 271.

23. Y. Wang, M. Guo, S. Wei, S. Yin, Y. Wang, Z. Song and M. R. Hoffmann, *Comput. Theor. Chem.*, 2014, **1049**, 28.
24. A. K. Weiss, T. S. Hofer, B. R. Randolf, A. Bhattacharjee and B. M. Rode, *Phys. Chem. Chem. Phys.*, 2011, **13**, 12173.
25. F. Hammami, A. Chebaane, M. Bahri and S. Nasr, *Eur. Phys. J. E. Soft Matter.*, 2013, **36**, 129.
26. A. Chebaane, F. Hammami, M. Bahri and S. Nasr, *J. Mol. Liq.*, 2012, **165**, 133.
27. A. Chebaane, F. Hammami, S. Nasr, M. Bahri and M.-C. Bellissent-Funel, *Eur. Phys. J. E*, 2015, **38**, 5.
28. I. P. Gerothanassis, I. N. Demetropoulos and C. Vakka, *Biopolymers*, 1995, **36**, 415.
29. W. Caminati, J. C. López, S. Blanco, S. Mata and J. L. Alonso, *Phys. Chem. Chem. Phys.*, 2010, **12**, 10230.
30. A. N. L. Batista, J. M. Batista Jr, V. S. Bolzani, M. Furlan and E. W. Blanch, *Phys. Chem. Chem. Phys.*, 2013, **15**, 20147.
31. S. W. Jacob and R. Herschler, *Cryobiology*, 1986, **23**, 14.
32. A. Giugliarelli, M. Paolantoni, A. Morresi and P. Sassi, *J. Phys. Chem. B*, 2012, **116**, 13361.
33. D. McCabe, M. D. O'Dwyer and M. D. Sickle-Santanello, *Arch Surg*, 1986, **121**, 1455.
34. R. J. Sengwa, S. Sankhla and V. Khatri, *Philos. Mag. Lett.*, 2010, **90**, 463.
35. J. M. M. Cordeiro and A. R. S. A. Bosso, *J. Mol. Liq.*, 2010, **154**, 36.
36. J. M. M. Cordeiro and A. K. Soper, *Chem. Phys.*, 2011, **381**, 21.
37. J. M. Cordeiro and A. K. Soper, *J. Chem. Phys.*, 2013, **138**, 044502.
38. A. Borges and J. M. Cordeiro, *Chem. Phys. Lett.*, 2013, **565**, 40.
39. H. J. C. Berendsen, J. R. Grigera, T. P. Straatsma and others, *J. Phys. Chem.*, 1987, **91**, 6269.
40. A. Luzar and D. Chandler, *J. Chem. Phys.*, 1993, **98**, 8160.
41. M. P. Allen and D. J. Tildesley, *Computer Simulation of Liquids*, 1987.
42. H. J. Berendsen, J. van Postma, W. F. van Gunsteren, A. DiNola and J. R. Haak, *J. Chem. Phys.*, 1984, **81**, 3684.
43. A. Chand, P. Chettiyankandy and S. Chowdhuri, *J. Mol. Liq.*, 2018, **269**, 241.
44. J. M. M. Cordeiro and A. K. Soper, *Chem. Phys.*, 2011, **381**, 21.
45. F. Hammami, H. Ghalla, A. Chebaane and S. Nasr, *Mol. Phys.*, 2015, **113**, 149.
46. J. M. M. Cordeiro and A. R. S. A. Bosso, *J. Mol. Liq.*, 2010, **154**, 36.
47. S. Chowdhuri and A. Chandra, *Chem. Phys. Lett.*, 2003, **373**, 79.
48. S. K. Pattanayak and S. Chowdhuri, *J. Phys. Chem. B*, 2011, **115**, 13241.
49. S. K. Pattanayak, N. Prashar and S. Chowdhuri, *J. Chem. Phys.*, DOI:10.1063/1.3578467.
50. A. Chandra and S. Chowdhuri, *J. Phys. Chem. B*, 2002, **106**, 6779.
51. S. Chowdhuri and A. Chandra, *J. Phys. Chem. B*, 2006, **110**, 9674.
52. J. P. Hansen and I. R. McDonald, "Theory of Simple Liquids", Academic Press, London, 1986.
53. L. Chen, T. Gross and H.-D. Lüdemann, *Z. Für Phys. Chem.*, 2000, **214**, 239.
54. L. Chen, T. Gross, H.-D. Lüdemann, H. Krienke and R. Fischer, *Naturwissenschaften*, 2000, **87**, 225.
55. I. Skarmoutsos and J. Samios, *Chem. Phys. Lett.*, 2004, **384**, 108.
56. A. Fratiello, *Mol. Phys.*, 1964, **7**, 565.
57. H. Weingärtner, M. Holz and H. G. Hertz, *J. Solut. Chem.*, 1978, **7**, 689.
58. A. Luzar and D. Chandler, *Nat. Lond.*, 1996, **379**, 53.
59. A. Chandra, *Phys. Rev. Lett.*, 2000, **85**, 768.
60. B. S. Mallik and A. Chandra, *J. Chem. Phys.*, DOI:10.1063/1.2403867.
61. D. Rapaport, *Mol. Phys.*, 1983, **50**, 1151.
62. I. P. Gerothanassis, I. N. Demetropoulos and C. Vakka, *Biopolymers*, 1995, **36**, 415.
63. F. Hammami, S. Nasr, M.-C. Bellissent-Funel and M. Oumezzine, *J. Phys. Chem. B*, 2005, **109**, 16169.